$H_3)SO_2OCH_2CF_3$, which was distilled bulb-to-bulb at ~75 °C was found in ~25% yield. 2,2,2-Trifluoroethyl fluorosulfate was reacted with $Me_3SiN(CH_3)CH_2CH_2N(CH_3)SiMe_3$ under similar conditions to give the sulfamate in approximately 30% yield.

The infrared spectrum is as follows: 2960 w, br, 1450 w, 1375 vs, br, 1290 vs, br, 1240 m, 1175 vs, br, 1100 w, 1050 vs, 1010 m, 970 vs, 900 vs, 865 m, 810 m, br, 720 w, 660 w, 605 w, 505 vs, 525 w cm^{-1}. The ^{19}F NMR and ^1H NMR spectra are as follows: a triplet at ϕ −74.13 (CF_3; $J_{CF_3-CH_2} = 8.1$ Hz); a quartet at δ 4.43 (CH_2CF_3) and two singlets at δ 3.05 (NCH_2) and 2.99 (CH_3). The EI mass spectrum contains the following peaks (*m/e*, species, %): 412, M^+, 0.06; 392, $M^+ - HF$, 0.2; 313, $M^+ - CF_3CH_2O$, 0.3; 312, $M^+ - CF_3CH_3O$, 4.2; 249, $M^+ - CF_3CH_2OSO_2$, 0.5; 248, $M^+ - CF_3CH_3OSO_2$, 6.0; 206, $CF_3CH_2OSO_2N(CH_3)CH_2^+$, 5.2; 205, $CF_3CH_2OSO_2N(CH_2)CH_2^+$, 100; 69, CF_3^+, 0.9; 64, SO_2, 2.8; 43, $CH_3NCH_2^+$, 16.8.

Anal. Calcd for $C_8H_{14}F_6N_2O_6S_2$: C, 23.30; H, 3.40; F, 27.67. Found: C, 23.22; H, 3.38; F, 27.5.

Acknowledgment is expressed to the donors of the Petroleum Research Fund, administered by the American Chemical Society, to the National Science Foundation (Grant CHE-8404974), and to the Air Force Office of Scientific Research (Grant 82-0247) for support of this research.

Registry No. $CF_3CH(CH_3)OSO_2F$, 99809-93-5; $CF_3C(CH_3)_2OSO_2F$, 99809-94-6; $(CF_3)_2CHOSO_2N(CH_3)_2$, 78162-70-6; $CF_3CH(CH_3)OSO_2N(CH_3)_2$, 99809-95-7; $CH_3NHCH_2CH_2NHCH_3$, 110-70-3; $CF_3CH_2OSO_2N(CH_3)CH_2CH_2N(CH_3)SO_2OCH_2CF_3$, 99809-96-8; $Me_3SiN(CH_3)CH_2CH_2N(CH_3)SiMe_3$, 1821-97-2; 1,1,1-trifluoro-2-propanol, 374-01-6; 2-(trifluoromethyl)-2-propanol, 507-52-8; 1,1,1,3,3,3-hexafluoroisopropyl fluorosulfate, 38252-04-9; 2,2,2-trifluoroethanol, 75-89-8; 1,1,1-trifluoroisopropyl 2,2,2-trifluoroethyl sulfate, 99809-97-9; bis(1,1,1-trifluoroisopropyl) sulfate, 99809-98-0; 2-(trifluoromethyl)propene, 374-00-5; 2,2,2-trifluoroethyl fluorosulfate, 66950-71-8.

Contribution from the Chemistry Department,
J. W. Goethe-Universität, D-6000 Frankfurt am Main, West Germany

Charge-Transfer and Electron-Transfer Properties of d^6 Metal Complexes with μ-Pyrazine. Mononuclear and Binuclear Manganese(I) Compounds

Renate Gross and Wolfgang Kaim*†

Received May 21, 1985

The electronic structures and the electron-transfer behavior of decacarbonyl(μ-pyrazine)dichromium(0) (**6**) and of tetracarbonyl(Cp)(μ-pyrazine)dimanganese(I) (**10**) (Cp = η^5-C_5H_5, η^5-$C_5H_4CH_3$, η^5-$C_5(CH_3)_5$) have been studied by electron spectroscopy, cyclic voltammetry, and high-resolution electron spin resonance (ESR) of the corresponding anion radicals. This combination of techniques allowed us to characterize the lowest unoccupied complex orbital as ligand-centered (π^*) and the first electronic transition as a metal-to-ligand charge-transfer (MLCT) process. However, in agreement with their pronounced light sensitivity, another close and apparently photoreactive excited state is indicated by the unexpectedly small *g* values of the anion radicals $\mathbf{10}^{-}\cdot$ of the binuclear Mn(I) complexes. While the persistence of these anion radical complexes increases with the number of methyl substituents at the cyclopentadienyl rings due to less facile cleavage of Cp^-, the reverse stability sequence has been observed for the photochemically induced ligand dissociation. A comparison of the binuclear organometallic complexes with related Fe(II), Ru(II), Os(II), and Ir(III) species suggests some similarity between the Mn(I) and Ru(II) systems according to a diagonal relationship and indicates a rather small splitting of d levels in the organometallic Mn(I) systems. Inclusion of mononuclear Mn(I) compounds **9** in the electrochemical and ESR studies reveals facile exchange processes such as the rapid formation of the more stable binuclear anion radicals $\mathbf{10}^{-}\cdot$ upon reduction. On the other side, the oxidation of all Mn(I)–pyrazine complexes was found to be irreversible in dimethylformamide (DMF) due to an ECE mechanism yielding solvent complexes of $CpMn(CO)_2$.

Pyrazine **1** is a small ligand with two special features: The presence of a low-lying molecular π^* orbital allows for back-bonding with suitable metal fragments and for facile one-electron reduction, and despite its low basicity toward non-back-bonding electrophiles, pyrazine may act as a linear bridge (μ-pyrazine) between two metals.[1]

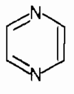

1

Both features of ligand **1** have been recognized and exploited by Creutz and Taube in their preparation of a series of Ru(II)/Ru(III) pentaammine complex **2**, including the first deliberately synthesized mixed-valence complex **2b**, the Creutz–Taube ion.[2] The unusual and still unresolved nature[3] of this complex has stimulated the synthesis of related binuclear pyrazine complexes with other metals in d^6 or d^5 configurations, among these being pentacyanoiron **3**[4] and osmium ammine complexes such as **4**[5] (group 8d),[48] pentachloroiridate complexes **5**[6] (group 9d), and pentacarbonylchromium, -molybdenum, and -tungsten complexes **6**–**8**[7–11] (group 6d).

Whereas mixed-valence oxidation states of the latter organometallic species were not reported, these compounds may undergo reversible one-electron reduction in nonaqueous media,[10] and in

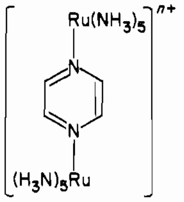

2a, $n = 4$
b, $n = 5$
c, $n = 6$

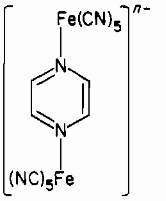

3a, $n = 6$
b, $n = 5$
c, $n = 4$

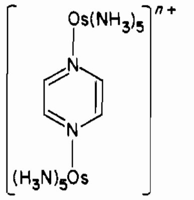

4a, $n = 4$
b, $n = 5$
c, $n = 6$

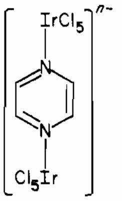

5a, $n = 4$
b, $n = 2$

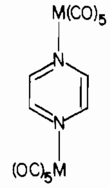

6, M = Cr
7, M = Mo
8, M = W

the cases of molybdenum and tungsten those ligand-centered anion radical complexes $\mathbf{7}^{-}\cdot$ and $\mathbf{8}^{-}\cdot$ and their P-donor substitution

---

† Karl Winnacker Fellow, 1982–1987.

(1) Kaim, W. *Angew. Chem.* **1983**, *95*, 201; *Angew. Chem. Int., Ed. Engl.* **1983**, *22*, 171.

(2) Creutz, C.; Taube, H. *J. Am. Chem. Soc.* **1969**, *91*, 3988; **1973**, *95*, 1086.

0020-1669/86/1325-0498$01.50/0 © 1986 American Chemical Society

products were characterized by means of high-resolution electron spin resonance (ESR).[12]

We report here the synthesis and properties of mono- and binuclear pyrazine complexes **9** and **10** with a d^6 metal system out of group 7d, viz., with the fragments $CpMn(CO)_2$.[13]

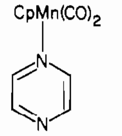

9a, $Cp = \eta^5\text{-}C_5H_5$
b, $Cp = \eta^5\text{-}C_5H_4CH_3$
c, $Cp = \eta^5\text{-}C_5(CH_3)_5$

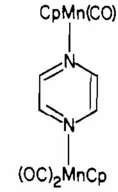

10a, $Cp = \eta^5\text{-}C_5H_5$
b, $Cp = \eta^5\text{-}C_5H_4CH_3$
c, $Cp = \eta^5\text{-}C_5(CH_3)_5$

The $CpMn(CO)_2$ fragments have been shown to stabilize many unusual ligands[14] such as carbenes,[15] vinylidenes,[16] carbynes,[17] heterocarbonyls,[18] ketenes,[19] dinitrogen,[20] or diazene (diimine).[21] Our interest in these Mn(I) species as coordination centers for unsaturated nitrogen ligands stems from their similarity to pentacarbonylmetal(0) fragments of group 6d. On the other hand, it was hoped that the study of the Mn(I) complexes of pyrazine might give some clues concerning the validity of a diagonal relationship[22] between Mn(I) and Ru(II), e.g. with respect to low-spin d^6 metal back-bonding toward π-electron-accepting ligands.

Our studies have focused on the charge-transfer and redox properties of systems **9** and **10**, and the results of these studies will be discussed in view of previous investigations of some related pyridine complexes.[23,24] We also report the redox behavior and the anion radical of decacarbonyl(μ-pyrazine)dichromium(0) (**6**), since previous attempts to obtain a persistent, well-characterized anion radical complex $\mathbf{6}^{-\cdot}$ have failed.[10,12]

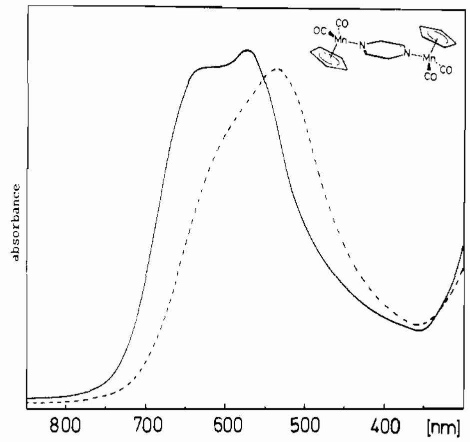

Figure 1. Electronic absorption spectra of **10a** in toluene (—) and DMF (---).

Experimental Section

Instrumentation. ^{1}H-NMR: Bruker WH 270, solvent or Me_4Si as internal standard. ESR: Varian E9, X band (9.5 GHz). Calibration of the spectra and *g* value determination were accomplished by using the double-cavity technique and the perylene radical anion in dimethoxyethane[25] as reference. The spectra were analyzed by computer simulation.[13,26] IR: Perkin-Elmer 283B, solution spectra in THF. UV/vis: Pye-Unicam SP 1800. MS: Varian MAT CH7. Cyclic voltammetry: PAR system 173/175, glassy-carbon working electrode, saturated calomel reference electrode (SCE), 0.1 M solution of tetrabutylammonium perchlorate in dry dimethylformamide (DMF) as electrolyte. Concentration of complexes during measurement was about 10^{-3} M, 100 mV/s scan rate. Elemental analyses have been performed by Mikroanalytisches Laboratorium Malissa & Reuter, Gummersbach, West Germany.

Preparations and spectroscopic measurements had to be carried out under an atmosphere of dry argon and under subdued light, since most of the pyrazine complexes proved to be light-sensitive. Photolyses were performed by using a falling-film photoreactor from Normag AG, Hofheim, West Germany, and a mercury lamp, Model TQ 150/Z1, from Quarzlampen GmbH, Hanau, West Germany.

Decacarbonyl(μ-pyrazine)dichromium(0) (6). The complex was prepared from 2 equiv of THF·$Cr(CO)_5$ and 1 equiv of pyrazine as reported.[10] The compound was purified by low-temperature (−30 °C) chromatography on Florisil (Merck); after elution of unreacted $Cr(CO)_6$ and of the mononuclear pentacarbonyl(pyrazine)chromium(0) with hexane, the binuclear species was collected as an orange-red zone with toluene. The IR spectrum in THF showed the expected three CO stretching frequencies (A_1, E, A_1) at 2062 (w), 1945 (s), and 1915 cm^{-1} (w); two,[9b] four,[10] or five[11b] bands were reported in previous studies. ^{1}H NMR (C_6D_6): δ 6.69 (s).

Tetracarbonyldicyclopentadienyl(μ-pyrazine)dimanganese(I) (10a). A solution of 2.04 g (10 mmol) of tricarbonylcyclopentadienylmanganese in 250 mL of THF was photolyzed at −40 °C to yield the red solvent complex $CpMn(CO)_2$·THF. This solution was then transferred into a Schlenk tube containing 0.25 g (3 mmol) of pyrazine (**1**), where the mixture was stirred overnight at room temperature to give a dark blue solution. After evaporation of the solvent and extraction of the residue with hexane to remove the bulk of unreacted tricarbonyl, the reaction mixture was chromatographed on a column (40 × 1.5 cm, Florisil) at −30 °C. While hexane eluted the remaining tricarbonyl and toluene eluted the reddish brown mononuclear complex **9a**, the binuclear complex was collected as a deep blue zone with THF. Recrystallization from hexane/THF at −28 °C yielded 0.36 g (27%) of **10a**. The compound is air-sensitive, soluble in toluene, benzene, THF, and DMF, and insoluble in saturated hydrocarbons. A mass spectrum gave the expected mole peak at *m/e* 432.

---

(3) (a) Creutz, C. *Prog. Inorg. Chem.* **1983**, *30*, 1. (b) Fürholz, U.; Bürgi, H. B.; Wagner, F. E.; Stebler, A.; Ammeter, J. H.; Krausz, E.; Clark, R. J. H.; Stead, M. J.; Ludi, A. *J. Am. Chem. Soc.* **1984**, *106*, 121. (c) Stebler, A.; Ammeter, J. H.; Fürholz, U.; Ludi, A. *Inorg. Chem.* **1984**, *23*, 2764.

(4) Felix, F.; Hauser, U.; Siegenthaler, H.; Wenk, F.; Ludi, A. *Inorg. Chim. Acta* **1975**, *15*, L7.

(5) Magnuson, R. H.; Lay, P. A.; Taube, H. *J. Am. Chem. Soc.* **1983**, *105*, 2507.

(6) Larèze, F. *C. R. Seances Acad. Sci., Ser. C* **1976**, *282*, 737; *Chem. Abstr.* **1976**, *85*, 28051*w*.

(7) Herberhold, M.; Süss-Fink, M. *Z. Naturforsch., B: Anorg. Chem., Org. Chem.* **1976**, *31*, 1489.

(8) Ernhoffer, R.; Shepherd, R. E. *J. Chem. Soc., Chem. Commun.* **1978**, 859.

(9) (a) Daamen, H.; van der Poel, H.; Stufkens, D. J.; Oskam, A. *Thermochim. Acta* **1978**, *34*, 69. (b) Daamen, H.; Stufkens, D. J.; Oskam, A. *Inorg. Chim. Acta* **1980**, *39*, 75.

(10) Pannell, K. H.; Iglesias, R. *Inorg. Chim. Acta* **1979**, *33*, L161.

(11) (a) Chun, S.; Palmer, D. C.; Mattimore, E. F.; Lees, A. J. *Inorg. Chim. Acta* **1983**, *77*, L119. (b) Lees, A. J.; Fobare, J. M.; Mattimore, E. F. *Inorg. Chem.* **1984**, *23*, 2709.

(12) (a) Kaim, W. *Inorg. Chim. Acta* **1981**, *53*, L151. (b) *Chem. Ber.* **1982**, *115*, 910. (c) *J. Organomet. Chem.* **1984**, *262*, 171.

(13) (a) Gross, R.; Kaim, W. *Angew. Chem.* **1984**, *96*, 610; *Angew. Chem., Int. Ed. Engl.* **1984**, *23*, 614. (b) Unsuccessful attempts to prepare **10b** were reported recently: Gaus, P. L.; Marchant, N.; Marsinek, M. A.; Funk, M. O. *Inorg. Chem.* **1984**, *23*, 3269.

(14) Caulton, K. G. *Coord. Chem. Rev.* **1981**, *38*, 1.

(15) Fischer, E. O.; Maasböl, A. *Chem. Ber.* **1967**, *100*, 2445.

(16) Nesmeyanov, A. N.; Aleksandrov, G.; Antonova, A.; Anisimov, K. N.; Kolobova, N.; Struchkov, Y. T. *J. Organomet. Chem.* **1976**, *110*, C36.

(17) Fischer, E. O.; Clough, R. L.; Stückler, P. *J. Organomet. Chem.* **1976**, *120*, C6.

(18) Fenster, A. E.; Butler, I. S. *Inorg. Chem.* **1974**, *13*, 915.

(19) Herrmann, W. A. *Angew. Chem.* **1974**, *86*, 345; *Angew. Chem., Int. Ed. Engl.* **1974**, *13*, 335.

(20) (a) Sellmann, D. *Angew. Chem.* **1972**, *84*, 549; *Angew. Chem., Int. Ed. Engl.* **1972**, *11*, 534. (b) Ziegler, M. L.; Weidenhammer, K.; Zeiner, H.; Skell, P. S.; Herrmann, W. A. *Angew. Chem.* **1976**, *88*, 761; *Angew. Chem., Int. Ed. Engl.* **1976**, *15*, 695.

(21) Sellmann, D. *J. Organomet. Chem.* **1972**, *44*, C46.

(22) Another example of a diagonal relationship between corresponding manganese and ruthenium oxidation states was noted recently in photosynthetic water oxidation systems: Lynch, M. W.; Hendrickson, D. N.; Fitzgerald, B. J.; Pierpont, C. G. *J. Am. Chem. Soc.* **1984**, *106*, 2041.

(23) Giordano, P. J.; Wrighton, M. S. *Inorg. Chem.* **1977**, *16*, 160. Most of the $CpMn(CO)_2(py)$ complexes reported were studied in solution and were not isolated.

(24) (a) Hershberger, J. W.; Klinger, R. J.; Kochi, J. K. *J. Am. Chem. Soc.* **1983**, *105*, 61. (b) Zizelman, P. M.; Amatore, C.; Kochi, J. K. *Ibid.* **1984**, *106*, 3771.

(25) Bolton, J. R. *J. Phys. Chem.* **1967**, *71*, 3702.

(26) Cf.: Kaim, W.; Bock, H. *J. Organomet. Chem.* **1979**, *164*, 281.

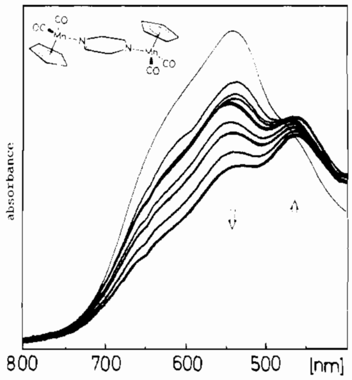

Figure 2. Dissociation of the binuclear complex **10a** (↓) into the mononuclear species **9a** (↑) and degradation products of $CpMn(CO)_2$ (no isosbestic behavior) as monitored by electron spectroscopy in THF. Spectra were recorded within 100 min after dissolution of **10a**.

Anal. Calcd for $C_{18}H_{14}Mn_2N_2O_4$: C, 50.02; H, 3.27; Mn, 25.42; N, 6.62. Found: C, 49.87; H, 3.40; Mn, 25.25; N, 6.48.

Tetracarbonylbis(methylcyclopentadienyl)(μ-pyrazine)dimanganese(I) (10b) and tetracarbonylbis(pentamethylcyclopentadienyl)(μ-pyrazine)dimanganese(I) (10c) were prepared in the same way by using tricarbonyl(methylcyclopentadienyl)- and tricarbonyl(pentamethylcyclopentadienyl)manganese as starting materials.

Dicarbonyl(cyclopentadienyl)-, dicarbonyl(methylcyclopentadienyl)-, and dicarbonyl(pentamethylcyclopentadienyl)(pyrazine)manganese(I) (9a–c) were obtained by similar procedures, either by reacting $CpMn(CO)_2{\cdot}THF$ and pyrazine in a 1:1 ratio or by collecting the mononuclear dissociation products by column chromatography of the binuclear species as described above.

Anal. Calcd for $C_{12}H_{11}O_2N_2Mn$ (**9b**): C, 53.35; H, 4.10; N, 10.37. Found: C, 53.30; H, 4.05; N, 9.86.

Complex anion radicals were prepared for ESR measurement by the following procedure. A dilute solution of the complex in THF was briefly brought into contact with vacuum-distilled potassium in an evacuated, sealed glass apparatus. The radical solution thereby formed was then transferred into a capillary extension of the apparatus, which served as the ESR cuvette. Although the anion radical $6^{-}\cdot$ was formed readily, this species showed rapid decay at room temperature (half-life of ca. 20 min). The concentration and persistency of the manganese complex radical anions depend critically on the methyl substitution at the cyclopentadienyl rings: $\mathbf{10a}^{-}\cdot$ is persistent only for some hours at ambient temperature, whereas $\mathbf{10c}^{-}\cdot$ proved to be stable for several days.

Results

Preparation, Stability, and Spectral Characterization. The binuclear chromium complex **6** and the manganese complexes **9a–c** and **10a–c** were prepared from photogenerated THF complexes by replacement of the THF through pyrazine in a thermal reaction, e.g. Scheme I. Since the second substitution step to the binuclear manganese complexes **10** is rather slow, reaction times of several hours at room temperature were necessary to obtain sufficient yields.[13] Conversely, the binuclear complexes **10** proved to be quite labile toward dissociation into the mononuclear derivatives, with visible light and coordinating solvents favoring such processes (eq 1).[8,11,23] This dissociation may be conveniently monitored, e.g.

$$\mathbf{10} + \text{solvent} \xrightarrow{h\nu} \mathbf{9} + CpMn(CO)_2{\cdot}\text{solvent} \qquad (1)$$

by UV/vis or ^1H NMR spectroscopy (cf. Figure 2); when the systems **10a–c** are compared, it appears that increasing methyl substitution at Cp favors this dissociative lability. The mononuclear complexes **9** are less sensitive toward further dissociation although they also show some degradation in solution after long exposure to daylight. Accordingly, the purification of the complexes **10**, especially their separation from the mononuclear species, had to be carried out via low-temperature chromatography under subdued light. Less gentle procedures led invariably to mixtures of products due to rapid dissociation as in (1). Nevertheless, the Mn(I) pyrazine complexes **9** and **10** can be isolated and stored for extended periods of time as solids.

Whereas the IR spectra of the complexes show that the carbonyl stretching frequencies of mono- and binuclear complexes are very similar (Table I), the ^1H NMR spectra in different solvents (Table II) reveal the tendency of the binuclear complexes toward dissociation. The chemical shifts indicate considerable charge-transfer interaction; the pyrazine protons in the complexes **10** show a characteristic, solvent-dependent high-field shift relative to those of the free ligand.

Table I. Carbonyl Infrared Stretching Frequencies ν_{CO} (cm^{-1}) of Mono- and Binuclear Mn(I)–Pyrazine Complexes in THF Solution

compd	ν_{CO}	compd	ν_{CO}
9a	1933, 1868	**10a**	1925, 1865
9b	1930, 1865	**10b**	1928, 1860
9c	1918, 1852	**10c**	1910, 1855

Table II. ^1H NMR Data for Mono- and Binuclear Mn(I)–Pyrazine Complexes in C_6D_6 and DMF-d_7

	chemical shifts			
compd	$\delta_{CH(pyr)}$	$\delta_{CH(Cp)}$	δ_{CH_3}	solvent
9a	7.23 (d) 8.01 (d) J = 3.0 Hz	4.03 (s)		C_6D_6
	8.24 (s) 8.93 (s)	4.61 (s)		DMF-d_7
9b	7.30 (d) 8.30 (d) J = 4.0 Hz	3.98 (s)	1.22 (s)	C_6D_6
	8.29 (d) 8.91 (d) J = 3.0 Hz	4.38 (s) 4.56 (s)	1.52 (s)	DMF-d_7
9c	7.27 (d) 8.02 (d) J = 1.7 Hz		1.40 (s)	C_6D_6
	8.24 (s) 8.71 (s)		1.62 (s)	DMF-d_7
10a	7.18 (s)	4.00 (s)		C_6D_6
	8.35 (s)	4.61 (s)		DMF-d_7
10b	7.21 (s)	3.89 (s)	1.22 (s)	C_6D_6
	8.37 (s)	4.38 (s) 4.50 (s)	1.52 (s)	DMF-d_7
10c	7.24 (s)		1.40 (s)	C_6D_6
	8.32 (s)		1.62 (s)	DMF-d_7

Electronic Spectra. The Mn(I) complexes **9** and **10** are intensely colored, the binuclear complexes being deep blue and the mononuclear derivatives being reddish brown in solution. A visible spectrum of complex **10a** in two different solvents (Figure 1) shows a rather intense band, which is split into at least two components due to the low symmetry of the $CpMn(CO)_2L$ fragment[23] and/or because of differently polarized transitions.[9b,11b] Spectral data in a polar medium (DMF) and in a nonpolar solvent (toluene) are given in Table III; however, exact extinction coefficients could not generally be determined due to the dissociative lability (eq 1) of the complexes in solution.[11b] An estimate of $\epsilon \sim 10^4$ for the most stable species **10a** is consistent with the MLCT (metal-to-ligand charge transfer) character of the dominant component in that band, as is the distinct solvent dependence, i.e., the hypsochromic shift in more polar solvents.[11,23,27] The mononuclear complexes **9** have absorption maxima more similar to those of related pyridine complexes;[23] their formation from binuclear precursors via dissociation 1 is illustrated in Figure 2.

Cyclic Voltammetry. The electrochemistry of the binuclear complexes **10** in DMF is characterized by reversible one-electron reduction and by irreversible oxidation (Figure 3). Although the oxidation occurs at rather low potentials, which are comparable to those of corresponding Fe(II) or Ru(II) species **2a** or **3a**,[2,4] there is clearly an ECE mechanism operating,[28] which yields the

---

(27) Manuta, D. M.; Lees, A. J. *Inorg. Chem.* **1983**, *22*, 3825. Kaim, W.; Kohlmann, S., manuscript submitted for publication.

(28) ECE refers to a mechanism in which an initial electrode process is followed by a chemical reaction forming a second electroactive species.

Table III. Low-Energy Charge-Transfer Absorption Maxima E_{MLCT} (eV)[a] of Mono- and Binuclear Mn(I)–Pyrazine Complexes and of Related Compounds[b]

compd with formal metal oxidn states			
no.	metal	E_{MLCT}	ref
2a	Ru(II)	2.27 (H_2O)	2
3a	Fe(II)	2.45 (H_2O)	4
4a	Os(II)	1.60 (H_2O)	5
5a	Ir(III)	2.60 (H_2O)	6
6	Cr(0)	2.41 (C_6H_6)	11b
7	Mo(0)	2.56 (C_6H_6)	11b
8	W(0)	2.43 (C_6H_6)	11b
9a[c]	Mn(I)	2.60 (C_7H_8);[d] 2.69 (THF); 2.75 (DMF)	this work
9b[c]	Mn(I)	2.61 (C_7H_8); 2.67 (THF); 2.72 (DMF)	this work
9c[c]	Mn(I)	2.45 (C_7H_8); 2.54 (THF); 2.62 (DMF)	this work
10a	Mn(I)	1.94, 2.14 (C_7H_8); 1.95 sh, 2.25 (THF); 1.96 sh, 2.29 (DMF)	this work
10b	Mn(I)	1.88 sh, 2.12 (C_7H_8); 1.92 sh, 2.18 (THF); 1.94 sh, 2.26 (DMF)	this work
10c	Mn(I)	1.80 sh, 2.03 (C_7H_8); 1.81 sh, 2.10 (THF); 1.82 sh, 2.16 (DMF)	this work

[a] For comparison with electrochemical potentials the transition energies are given in eV (1 eV = 8066 cm^{-1}). [b] Solvents are given in parentheses. [c] Long-wavelength shoulders indicated by asymmetry of the bands. [d] Toluene.

Table IV. Anodic and Cathodic Peak Potentials E_{pa} and E_{pc} (V vs. SCE) of Mono- and Binuclear Mn(I)–Pyrazine Complexes[a] and of Related Compounds

compd with formal metal oxidn state			
no.	metal	E_{pa}	E_{pc}
2a	Ru(II)	+0.15[b] (r)	c
4a	Os(II)	−0.65[b] (r)	c
6	Cr(0)	+1.10 (ir)	−1.05 (ir)
9a	Mn(I)	+0.39 (ir)[d]	−1.59 (ir)[e]
9b	Mn(I)	+0.36 (ir)[d]	−1.61 (ir)[e]
9c	Mn(I)	+0.29 (ir)[d]	−1.70 (ir)[e]
10a	Mn(I)	+0.41 (ir)[d]	−1.36 (r)
10b	Mn(I)	+0.37 (ir)[d]	−1.37 (r)
10c	Mn(I)	+0.30 (ir)[d]	−1.42 (r)

[a] Values from cyclovoltammetry in DMF/0.1 M $Bu_4N^+ClO_4^-$, scan rate 100 mV/s. Redox processes are characterized as reversible (r) or irreversible (ir) according to established criteria (ΔE, i_a/i_c). [b] References 2 and 5; measurements in aqueous solutions, potentials recalculated vs. SCE (+0.241 V vs. NHE). [c] Not reported; cf., however, ref 37. [d] Formation of the reversible couple $[CpMn(CO)_2 \cdot DMF]^{0/+}$; E(**a**) = +0.14 V, E(**b**) = +0.11 V, and E(**c**) = −0.06 V vs. SCE. [e] Formation of the corresponding binuclear complex anion.

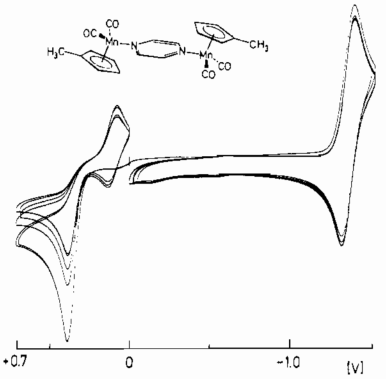

Figure 3. Cyclic voltammograms for oxidation and reduction of complex **10b** in DMF/0.1 M $Bu_4N^+ClO_4^-$ (scan rate 100 mV/s). Repeated scans illustrate the reversibility (reduction) and the ECE mechanism (oxidation).

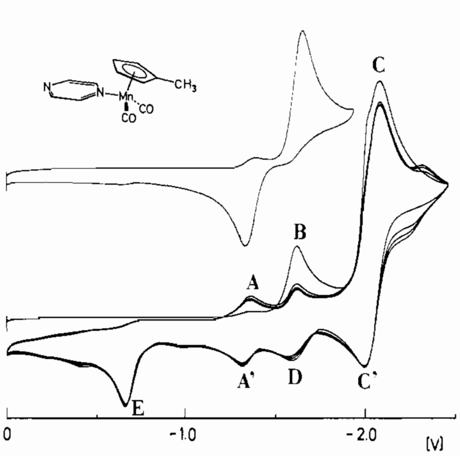

Figure 4. Cyclic voltammogram for the reduction of complex **9b** in DMF/0.1 M $Bu_4N^+ClO_4^-$, scan rate 100 mV/s. The single scan (top) shows the rapid formation of **10b**$^{-}\cdot$ after the reduction of **9b**; cycling in a wider potential range (bottom) reveals other fragmentation products. Peak potentials of the following redox processes are indicated: (A, A') cathodic reduction and anodic reoxidation of **10b**; (B) cathodic reduction of **9b**; (C, C') cathodic reduction and anodic reoxidation of pyrazine **1**; (D) anodic oxidation of $[(\eta^5\text{-}C_5H_4CH_3)Mn(CO)_2(DMF)]^-$ (cf. Scheme II); (E) probably anodic oxidation of dissociated $(C_5H_4CH_3)^-$ (cf. ref 32).

electrochemically reversible couple $[CpMn(CO)_2 \cdot DMF]^{0/+}$. Reversible couples of this kind and their function in electrocatalytic ligand-exchange reactions have recently been studied by Kochi and co-workers;[24] in agreement with the similar solvent properties of acetonitrile and DMF, the potentials of the two $[CpMn(CO)_2 \cdot solvent]$ complexes are comparable (Table IV). On the other hand, the reduction of the binuclear complexes **10** is reversible at potentials that are markedly higher than the reduction potential of the free ligand but that are more negative than the reduction peak potential of the chromium complex **6**. The latter exhibits only irreversible electrochemical reduction, which relates to difficulties in obtaining a persistent anion radical **6**$^{-}\cdot$. Such a dissociative behavior corroborates recent results obtained for pentacarbonyl(pyridine) metal complexes.[29]

A remarkable electrochemical behavior has been noted for the mononuclear complexes **9**, exemplified here by the methylcyclopentadienyl derivative **9b**. The reduction of this species occurs at a more negative potential than the reduction of the binuclear derivative **10b**; however, this reduction of **9b** is followed in the reverse scan by the reoxidation of the binuclear anion radical **10b**$^{-}\cdot$; i.e., there must have been a rapid exchange reaction yielding the more stable binuclear radical anion (Figure 4A). Additional cycles over a wider potential range show a typical steady-state situation with reduction peaks of the mono- and binuclear complex and of the pyrazine ligand and with oxidation peaks of the pyrazine anion, of the binuclear complex anion, and of some further fragments of the $CpMn(CO)_2$ moiety (Figure 3B). These latter oxidation peaks have also been observed in the (irreversible) reduction of tricarbonyl(methylcyclopentadienyl)manganese itself,[30] and in analogy with the electrochemical reduction behavior of $Cr(CO)_6$,[31] some of them may be tentatively assigned to the oxidation of $[CpMn(CO)_2 \cdot DMF]^{-}\cdot$ ($E_{ox}{}^{p} = -1.65$ V vs. SCE), of Cp^- ($E_{ox}{}^{p} \sim -0.6$ V vs. SCE),[32] and of other metal-containing species.

Similar sequences were observed for the other two mononuclear complexes **9a** and **9c**; the amount of fragmentation was found to decrease with increasing methyl substitution at Cp. Redox po-

---

(29) (a) Kaim, W. *Inorg. Chem.* **1984**, *23*, 504. (b) *Z. Naturforsch., B: Anorg. Chem., Org. Chem.* **1984**, *39*, 801.

(30) Unpublished results. Cf. also: Würminghausen, T.; Sellmann, D. *J. Organomet. Chem.* **1980**, *199*, 77.

(31) Pickett, C. J.; Pletcher, D. *J. Chem. Soc., Dalton Trans.* **1976**, 749.

(32) An oxidation peak potential of cyclopentadienide anion of −0.37 V vs. SCE has been measured at −62 °C in HMPA/THF: Jaun, B.; Schwarz, J.; Breslow, R. *J. Am. Chem. Soc.* **1980**, *102*, 5741.

Scheme I

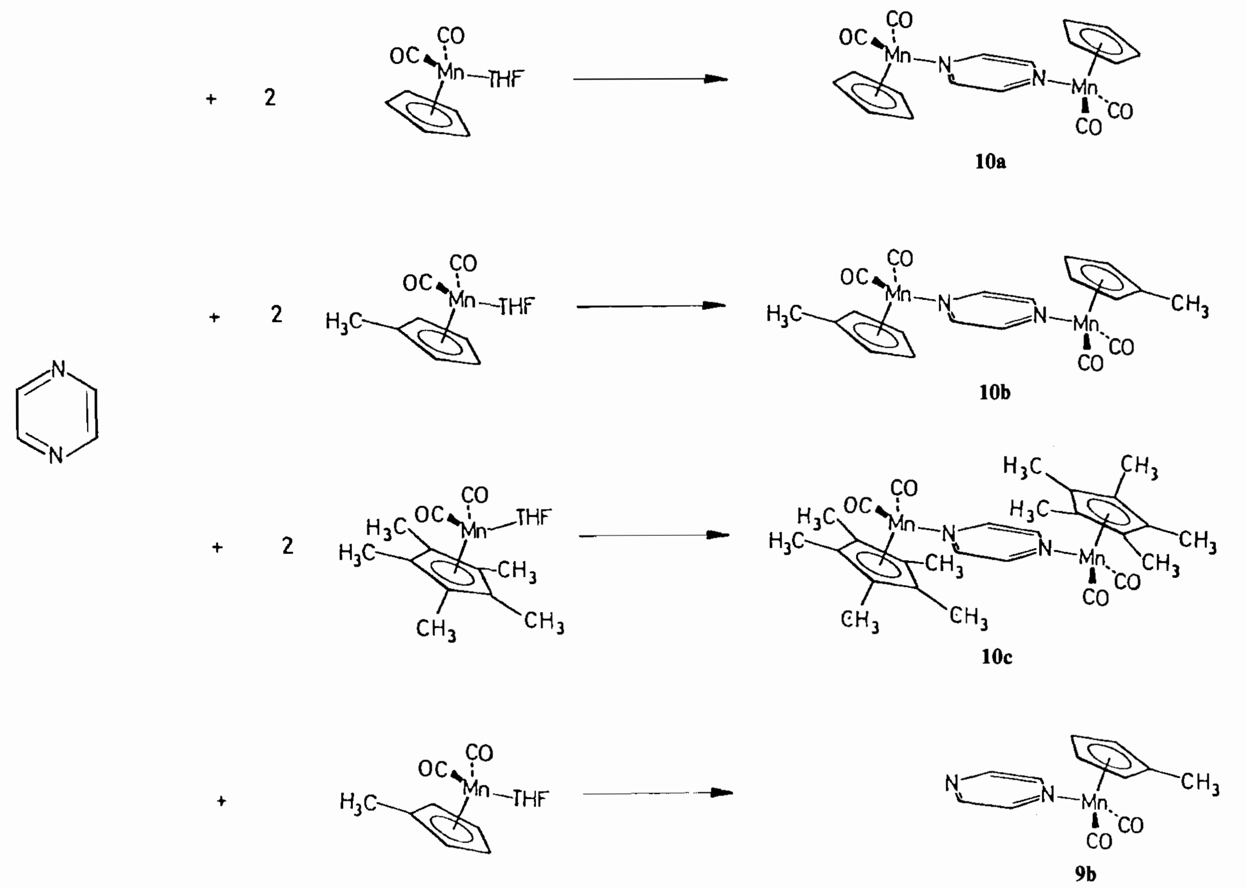

Table V. Electron Spin Resonance Parameters for Binuclear d^6 Metal Complexes of the Pyrazine Anion Radical[a]

radical	coordinated metal	g	$a_H{}^{CH}$	$a_{^{14}N}$	$a_M{}^b$	$a_M/A_M{}^{iso\,c}$	ξ^d
1$^{-}\cdot$	none	2.0035	264	718			
6$^{-}\cdot$	Cr(0)	2.0035	246	859	70	0.0031	223
7$^{-}\cdot$	Mo(0)	2.0042	253	818	150	0.0033	552
8$^{-}\cdot$	W(0)	2.0061	254	823	286	0.0053	2089
10a$^{-}\cdot$	Mn(I)	1.9999	225	881	733	0.0067	254
10b$^{-}\cdot$	Mn(I)	1.9997	226	863	750	0.0069	254
10c$^{-}\cdot$	Mn(I)	1.9994	228	864	763	0.0070	254

[a] Measurements in THF solutions at room temperature, K$^+$ as counterion; hyperfine coupling constants a in μT (=0.01 G). [b] ^{53}Cr 9.5% natural abundance, $I = {}^3/_2$; ^{95,97}Mo 25.4%, $I = {}^5/_2$; ^{183}W 14.3%, $I = {}^1/_2$; ^{55}Mn 100%, $I = {}^5/_2$. [c] $A_M{}^{iso}$ is the isotropic hyperfine coupling constant of the metal M from ref 41. [d] Spin–orbit coupling constants (cm^{-1}) from ref 41.

tentials of the compounds investigated and of related pyrazine complexes are summarized in Table IV.

Electron Spin Resonance of Complex Anion Radicals. Encouraged by the electrochemically reversible formation of the anion radicals **10$^{-}\cdot$** we have succeeded in obtaining these persistent species also by chemical reduction in THF solution. Well-resolved ESR spectra have been recorded for the radicals **10$^{-}\cdot$** (Figure 5) and also for the pentacarbonylchromium analogue **6$^{-}\cdot$** although the latter species was not very persistent at room temperature. The persistency of the radical complexes **10a–c$^{-}\cdot$** depends markedly on the substitution at the cyclopentadienyl rings. Introduction of methyl groups kinetically stabilizes the anion radical complexes despite the fact that the reduction becomes more difficult (Table IV).

The ESR data in Table V show unusually small g values (g < 2) for the manganese radical complexes; in contrast, g of pentacarbonylmetal analogues with Cr, Mo, or W is always larger than that of the free electron (g_e = 2.0023).[33] Hyperfine coupling could be detected with the protons and the nitrogen nuclei of the pyrazine ligand and with the two manganese nuclei (^{55}Mn, 100% natural abundance, $I = {}^5/_2$), any hyperfine interaction between the unpaired electron and the protons at the cyclopentadienyl rings must be smaller than 5 μT. Corroborating the electrochemical results (Figure 4), chemical reduction of the mononuclear complexes **9** yielded the binuclear anion radicals **10$^{-}\cdot$**.[13]

Discussion

Preparation and purification of the manganese(I) complexes **9** and **10** were affected by their propensity to dissociate in solution (eq 1). Although such a behavior parallels the lability encountered with, e.g., related binuclear pentacarbonylmolybdenum(0) species **7**,[8] the situation is aggravated for the CpMn(CO)$_2$ complexes because of their distinct light sensitivity. In fact, related pyridine complexes CpMn(CO)$_2$(py) were shown to undergo efficient photosubstitution (quantum yields $\Phi \sim 0.25$) after irradiation into the long wavelength band system; such a behavior, which is considered incompatible with a pure MLCT excited state, has been interpreted by Giordano and Wrighton[23] with a nearby substitutionally reactive ligand field (LF, d $\rightarrow$ d) excited state.

Although pyrazine is a rather weak base (pK_{a_1} = 0.65, pK_{a_2} = −6), the basicity of the second nitrogen center may be raised considerably by electron back-transfer from a coordinated low-

---

[33] For a discussion of g values in anion radical complexes, cf.: Kaim, W. *Inorg. Chem.* **1984**, *23*, 3365.

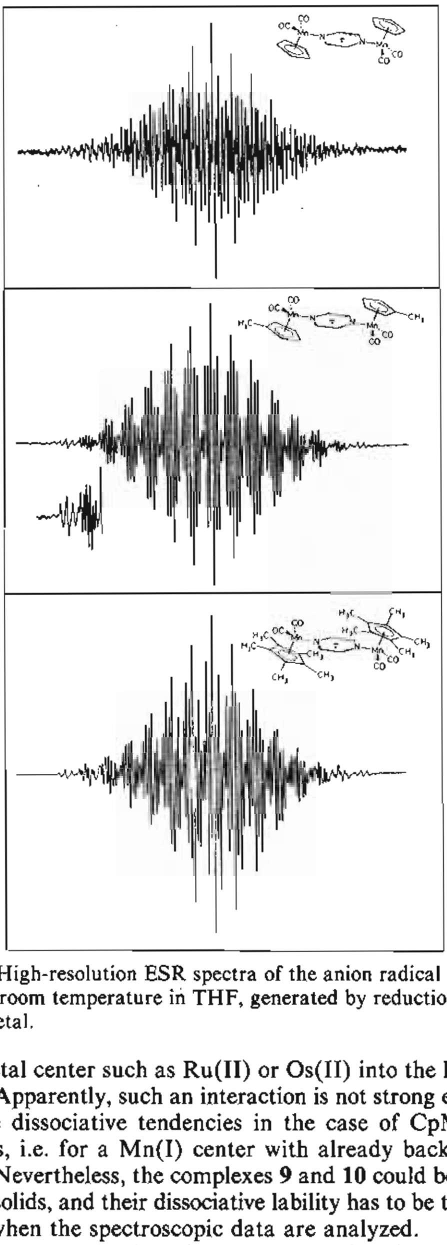

Figure 5. High-resolution ESR spectra of the anion radical complexes **10a–c**$^{-\cdot}$ at room temperature in THF, generated by reduction with potassium metal.

valent metal center such as Ru(II) or Os(II) into the ligand π^* level.[1,3a] Apparently, such an interaction is not strong enough to offset the dissociative tendencies in the case of CpMn(CO)$_2$ fragments, i.e. for a Mn(I) center with already back-bonding ligands. Nevertheless, the complexes **9** and **10** could be isolated as stable solids, and their dissociative lability has to be taken into account when the spectroscopic data are analyzed.

A first characterization of the complexes **9** and **10** by optical spectroscopy shows that the mononuclear compounds **9** have absorption maxima similar to those of complexes of CpMn(CO)$_2$ with 4-acceptor-substituted pyridines.[23] The binuclear complexes, however, display a further bathochromic shift, and a comparison of the long-wavelength absorptions in bis(d^6 metal) complexes with μ-pyrazine in Table III[34] demonstrates the very low transition energies of these Mn(I) complexes. All of these absorptions have been attributed to metal (dπ)-to-ligand (π^*) charge-transfer (MLCT) transitions. This assignment is based on the intensity and on the solvent dependence of the bands,[27,35a] as well as on NMR chemical shifts, which are indicative of strong charge-transfer interactions. ESR evidence for the π character of the lowest unoccupied molecular orbital (LUMO)[12,29,33] is given below. The two discernible bands in the visible spectrum of the binuclear Mn(I) complexes **10** (Figure 1) arise either because of the strong perturbation of octahedral symmetry around the manganese centers[23] or because of differently polarized transitions[9b] as has been observed for the related pentacarbonyltungsten complex **8** in certain solvents.[11b] Table III shows that the Mn(I) complexes **10** absorb at rather low energies when compared to pentacarbonylmetal complexes of group 6d or to the Fe(II), Ru(II), and Ir(III) complexes **3a**, **2a**, and **5a**, which, however, were studied in aqueous solution. The Mn(I) complexes **10** are only surpassed by the osmium pentaammine system **4**, which also exhibits strong delocalization of the d^6/d^5 mixed-valence species.[5]

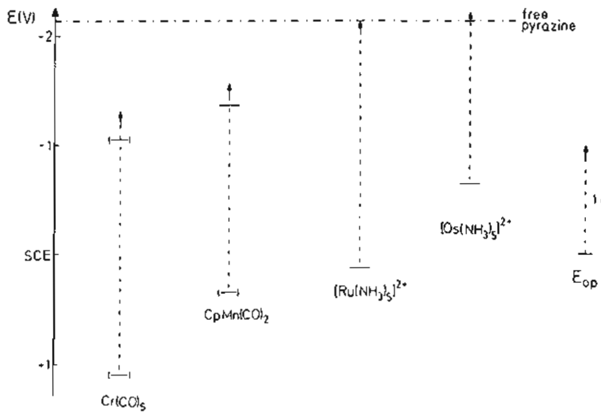

Figure 6. Redox potential diagram for binuclear pyrazine complexes $[(\mathbf{1})(\mathrm{ML}_n)_2]$ with different metal fragments ML$_n$. Redox levels in parentheses refer to irreversible processes; data for the organometallic species were determined in DMF, and values for the $(\mathrm{NH_3})_5\mathrm{M}^{2+}$ complexes were measured in water.[2,5] Charge-transfer absorption energies (band maxima in eV) are indicated by vertical broken arrows.

Further insight as to what kind of changes determine these different absorption energies of the complexes may be gained by electrochemistry. To a first approximation, the redox potentials should allow an assessment of the relative energies of the frontier orbitals HOMO and LUMO, and especially the difference between the oxidation and reduction potentials of a given system should, in a one-electron scheme, correlate with the optical HOMO–LUMO transition observed. Such correlation between optical and electrochemical data, although still in its beginnings, may provide useful additional insight[35b,36] due to the complementarity of the two experiments. Although some of the redox processes of compounds **6** and **10** are not reversible under the conditions of measurement employed here, the data in Tables III and IV and their visual representation in Figure 6 demonstrate the reasonable success of this approach for both types of organometallic complexes. The somewhat larger energies of the optical transitions (band maxima) can be attributed to a variety of factors such as resonance and exchange energies[36] and to the Franck–Condon effect according to eq 2 where χ values are

$$E_{\mathrm{op}} = \Delta E_{\mathrm{ox/red}} + \chi \qquad (2)$$

contributions to the Franck–Condon energy from intra- and intermolecular vibrations in the medium.[36]

From Figure 6 it is evident that the (metal-centered) HOMO is shifted to more negative potentials on going from the Cr(0) via the Mn(I) and Ru(II) to the Os(II) complex, notably, the oxidation potentials of the CpMn(CO)$_2$ and [Ru(NH$_3$)$_5$]$^{2+}$ systems are quite close; incidentally, Mn^{n+} and Ru$^{(n+1)+}$ are connected by a diagonal relationship in the periodic system.[22] On the other hand, the reduction potentials that may be associated with the energy of the ligand-centered LUMO show a smaller shift toward negative potentials. Although the reduction potentials of the ruthenium(II) and -osmium(II) pentaammine species have not been determined in aqueous solution,[37] there is less net change with respect to the reduction level of the free pyrazine ligand and the oxidation

---

[34] A sequence of d^6 metal fragments, based on MLCT spectral data of mononuclear pyridine and pyrazine complexes but without inclusion of Mn(I) species, has been published recently: Johnson, C. R.; Shepherd, R. E. *Inorg. Chem.* **1983**, *22*, 2439.

[35] Lever, A. B. P. "Inorganic Electronic Spectroscopy", 2nd ed.; Elsevier: Amsterdam, 1984: (a) p 203; (b) pp 776–779.

[36] The approximations required for such correlations have been pointed out by: Curtis, J. C.; Sullivan, B. P.; Meyer, T. J. *Inorg. Chem.* **1983**, *22*, 224. Cf. also: Ohsawa, Y.; Hanck, K. W.; DeArmond, M. K. *J. Electroanal. Chem. Interfacial Electrochem.* **1984**, *175*, 229. Dodsworth, E. S.; Lever, A. B. P. *Chem. Phys. Lett.* **1985**, *119*, 61.

[37] A reversible two-electron reduction at −1.44 V vs. SCE has been observed for $[(\mathbf{1})\mathrm{Ru(NH_3)_5}]^{2+}$ in alkaline solution: Lim, H. S.; Barclay, D. J.; Anson, F. C. *Inorg. Chem.* **1972**, *11*, 1460.

potential of the metal fragment largely determines the energy of the MLCT transition. The relatively high lability of the organometallic complexes **6** and **10** may be viewed as resulting from a mismatch between dominant π back-bonding and only weak σ interaction, whereas a higher metal oxidation state such as in the Fe(II), Ru(II), or Os(II) species favors σ bonding while still allowing for back-donation from the low-lying metal d orbitals. For the Ir(III) species the situation becomes less favorable again because of diminished back-bonding and because of their very high oxidation potentials, which lie outside of the range tolerable in aqueous solution.[6]

Besides being an assessment of the relative levels of the frontier orbitals, the cyclic voltammetric experiments also reveal much about the reactivities of the different oxidation states in solution. Thus, the oxidation of the binuclear Mn(I) complexes **10** clearly occurs via an ECE mechanism (Figure 2). Oxidized **10**, i.e. $\mathbf{10}^{+\cdot}$, dissociates rapidly to give the radical cation of the solvent complex $[\mathrm{CpMn(CO)_2{\cdot}DMF}]^{+\cdot}$, which undergoes reversible reduction on the time scale of the cyclic voltammetry experiment. The potential of this latter process ($E = +0.11$ V vs. SCE for Cp = $C_5H_4CH_3$) is comparable to the oxidation potential of the acetonitrile complex in CH_3CN ($E = +0.26$ V recalculated vs. SCE),[24a] in agreement with the similar solvation properties of both solvents. Also, the oxidation peak potentials of the mono- and binuclear pyrazine complexes **9b** and **10b** ($E_{ox}^{p} \sim +0.35$ V at 100 mV/s scan rate) are close to that of the corresponding pyridine complex $[(C_5H_4CH_3)Mn(CO)_2{\cdot}(C_5H_5N)]$ for which Hershberger, Klingler, and Kochi[24a] have measured $E_{ox}^{p} = +0.21$ V (recalculated vs. SCE) in acetone. They have also shown that electron-transfer-induced substitution mechanisms in the $\mathrm{CpMn(CO)_2L}$ series can occur in a chain fashion (electrocatalysis), which ensures effective attainment of the thermodynamical reaction equilibrium; in the competition between pyrazine and DMF used as solvent in large excess, the two-step equilibrium (3) is shifted to the right side.

$$(\mathbf{1})[\mathrm{CpMn(CO)_2}]_2 + 2\mathrm{DMF} \rightleftharpoons \mathbf{1} + 2\mathrm{CpMn(CO)_2(DMF)} \qquad (3)$$

This fact has precluded investigation of the possibility of formation of a Mn(II)/Mn(I) mixed-valence complex, which would be analogous (d^6/d^5) to the Creutz–Taube ion;[2,3a] it seems that other, more electrophilic manganese fragments and less coordinating solvents are required to achieve such a goal.

Electrochemical reduction of the complexes **10** in DMF proceeds in a straightforward reversible one-electron transfer (Figure 2). As in the case of the oxidation peak potentials, the reduction potentials decrease slightly with an increasing number of (electron-donating) methyl substituents on the cyclopentadienyl rings. A very interesting behavior is noted upon electrochemical (and chemical) reduction of the mononuclear species **9**. Although the reduction occurs at a more negative potential than the reduction of the binuclear analogues **10**, the reoxidation is clearly that of $\mathbf{10}^{-\cdot}$ on the time scale of the cyclic voltammetry experiment; apparently, rapid dissociation of reduced **9** and formation of the more stable radical anion $\mathbf{10}^{-\cdot}$ must have taken place. If the scan range of the CV experiment is extended further into the negative potential region one can find other species as parts of a general electron-transfer/dissociation scheme (Figure 4, Scheme II). Reversible reduction of free pyrazine **1** is observed (Figure 4B) as well as the reoxidation of some metal fragment cleavage products, some of which, in analogy with the electrochemical behavior of carbonylchromium, -molybdenum, and -tungsten systems[29,31] are tentatively identified as $[\mathrm{CpMn(CO)_2(DMF)}]^{-\cdot}$ and Cp^{-}.[32] These latter peaks also show up in the oxidative back scan of the irreversible reduction of tricarbonyl(methylcyclopentadienyl)manganese ($E_{red}^{p} = -2.4$ V vs. SCE).[30]

The observation of free Cp^{-} ions formed after exhaustive reduction of the complexes **9** and **10** already indicates that the stability of the anion radicals $\mathbf{10}^{-\cdot}$ might be limited by their propensity to lose a cyclopentadienide ion. In agreement with such an expectation, the persistence of the anion radicals $\mathbf{10}^{-\cdot}$ increases markedly in the series $\mathbf{10a}^{-\cdot} < \mathbf{10b}^{-\cdot} < \mathbf{10c}^{-\cdot}$, i.e. with an increasing number of methyl substituents at the Cp rings and hence a decreasing tendency to accept a negative charge. Accordingly, the extent of fragmentation during the cyclic voltammetry experiment (cf. Figure 4B) is diminished in the order given above; the thermodynamic stabilities, as reflected in the reduction potentials of the complexes **10** show, however, an opposite behavior, with the permethyl derivative **10c** being most difficult to reduce.

Scheme II. Redox/Coordination Scheme[a]

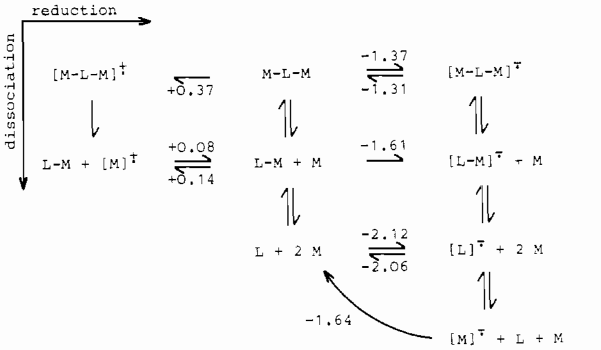

[a] For the system L = pyrazine, M = $(\eta^5\text{-}C_5H_4CH_3)Mn(CO)_2$ (solvated). Data taken from cyclic voltammetry (cf. Figures 3 and 4) in DMF at 100 mV/s scan rate, potentials in V vs. SCE.

We have already, in some instances,[12,13,29,33,38] suggested that the formation of persistent ligand-centered anion radicals and their detection by high-resolution ESR serves to establish the π^* character of the LUMO of a complex, which, in turn, may constitute support for the MLCT assignment of the lowest electronic transition. Such assignments are not always straightforward by other spectroscopic means, and in addition, high-resolution ESR can provide detailed information on the distribution of the unpaired electron in that π^* orbital before and after coordination.

Table V shows that, relative to free pyrazine radical anion, the proton coupling constants are diminished in the complex anion radicals. The translation of this effect via the McConnell equation[39]

$$a_H^{CH} = Q\rho_C^{\pi} \qquad (4)$$

where a_H = proton coupling constant (1 μT = 10^{-2} G), Q = constant, and ρ_C^{π} = π spin population at carbon π center, into a flow of unpaired electron density from the pyrazine carbon centers toward the metal coordination sites means that the interactions between the metal fragments and the reduced ligand increase along the series given in Table V, viz. on going from the Mo and W pentacarbonyl complexes via the Cr pentacarbonyl and the Mo and W tetracarbonyl phosphane species to the manganese complexes $\mathbf{10}^{-\cdot}$. The shift of unpaired electron density is also evident from the large ^{14}N coupling constants of the complexes and from the (relatively) increasing metal hyperfine splitting. Applying eq 4 with $Q = 2300$ μT,[39] the complexation of pyrazine anion radical $\mathbf{1}^{-\cdot}$ by two $\mathrm{CpMn(CO)_2}$ fragments leads to a total loss of π spin population of $4(\Delta a/Q) = 4(40\ \mu T/2300\ \mu T) = 6.5\%$ at the four pyrazine carbon π centers.

In the series of group 6d pentacarbonylmetal complexes, the smallest ^1H coupling is displayed by the chromium complex, probably an effect of the smaller distance between the first-row transition metal and the spin-bearing pyrazine π system; several details of the highly resolved ESR spectra such as metal isotope, carbonyl carbon,[12a,b] and ^{31}P hyperfine couplings[12c] have been interpreted in terms of a σ^*_{M-X}/π^* hyperconjugative mechanism, which is certainly more effective at smaller distances. Apparently, this interaction is even larger in the Mn(I) radical complexes $\mathbf{10}^{-\cdot}$ although the species may still be regarded as ligand-centered radical ions. At present, we cannot specify what particular kind of interaction is responsible for this observation, certainly, the higher formal oxidation state (+I) of the metal plays a role. However, at present neither the conformation of compounds **9** and

---

[38] Kaim, W.; Kasack, V. *Angew. Chem., Int. Ed. Engl.* **1982**, *21*, 700; *J. Organomet. Chem.* **1984**, *264*, 317.

[39] McConnell, H. M. *J. Chem. Phys.* **1956**, *24*, 632.

Scheme III. Alternatives of Relative MO Ordering in Radicals[a]

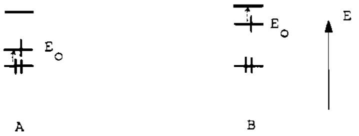

[a] According to eq 5, situation A is associated with $g > g_e$, whereas situation B leads to $g < g_e$.

10 nor a detailed calculation of the electronic structure is available. An interesting fact is the lack of hyperfine coupling for the cyclopentadienyl ring protons, indicating that the electron added does not prefer to reside in those negatively charged ligands.

We have recently shown[33] that the g values of such radical ion complexes, the "chemical shifts", are a very useful source of information concerning the electronic structure of the complex. The deviation of g from the free electron value of $g_e = 2.0023$ may be attributed to the admixture of higher (triplet) excited states to the doublet radical ground state. According to a first approximation,[40] $g = g_e + \Delta g$ can be expressed as a function of the spin–orbit coupling constants ξ_k of the participating atoms and of the energy differences $E_n - E_0$ between the singly occupied molecular orbital (E_0) and the other completely occupied or unoccupied MOs (E_n; cf. Scheme III and eq 5; $\mathbf{L}$ = angular

$$g = g_e - \tfrac{2}{3}\sum_i \sum_n \sum_{k,j} \frac{\langle \psi_0 | \xi_k \mathbf{L}_{ik} \delta_k | \psi_n \rangle \langle \psi_n | \mathbf{L}_{ij} \delta_j | \psi_0 \rangle}{E_n - E_0} = g_e + \Delta g \qquad (5)$$

momentum operator). Since the energy differences are in the denominator of eq 5, only the neighboring levels need be considered as contributing significantly to Δg; however, there are two alternatives regarding the sign of Δg. For dominating $E_n < E_0$ (Scheme IIIA), g becomes larger than $g_e = 2.0023$, whereas for $E_n > E_0$ (Scheme IIIB), g decreases relative to g_e.[33]

These effects are most conspicuous for paramagnetic transition metal ions such as d^9 systems (case A, $g > g_e$) or d^1 systems (case B, $g < g_e$) where the difference between d levels is much smaller than the gap between d orbitals and the next filled or unfilled s or p levels; however, this approach may also be employed for delocalized organometallic radical complexes.

In most anion radical complexes with group 6d metal carbonyls, including the species $6^{-}\cdot$, $7^{-}\cdot$, and $8^{-}\cdot$,[12b] there is a pattern of g corresponding to g(ligand) ~ g(Cr complex) < g(Mo complex) << g(W complex),[33] the large increase in g for the tungsten complex being due to the high spin–orbit coupling factor of tungsten (Table V).[41] Only for group 6d metal carbonyl complexes with the binucleating chelate ligand 2,2′-bipyrimidine has this order found to be reversed.[33]

In the present case of binuclear pyrazine complexes with $CpMn(CO)_2$ fragments, the g values are quite small and do not even exceed $g = 2$. For these Mn(I) radical anion complexes the (negative) deviation of about −0.0038 from $g = 2.0035$ of the free ligand anion radical $1^{-}\cdot$ is even larger than the positive shift of 0.0026 that has been noted for $8^{-}\cdot$,[12] a complex containing two coordinated tungsten atoms with their large spin–orbit coupling constant.[41] This remarkable result indicates a situation according to Scheme IIIB; i.e., there is a second unoccupied orbital close to the pyrazine ligand π^* level so that the predominant contribution to Δg is from a nearby excited state, which arises from the excitation of the odd electron into that next unoccupied orbital. Such an explanation of the unexpected g values of the radical ions $10^{-}\cdot$ supports Giordano and Wrighton's interpretation of the d → d or ligand field (LF) character of a low-lying excited state in some related photoreactive pyridine complexes with the $CpMn(CO)_2$ fragments.[23] Due to the lower extinctions of LF transitions such features are likely to be obscured by charge-transfer bands, and exact positioning of excited states in the binuclear pyrazine complexes **10** must be left to a detailed photochemical study.[42]

Scheme IV. Relative Frontier MO Levels in (Pyrazine)bis(d^6 metal fragment) Complexes as Deduced from Electrochemistry, ESR and Absorption Spectroscopy

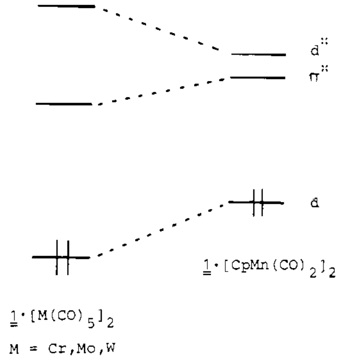

For the related bis(pentacarbonyltungsten) complex **8**, Lees and co-workers[11b] have demonstrated that irradiation into the LF band (which is separated from the long-wavelength MLCT transitions) leads to quite effective metal–pyrazine cleavage. It seems, therefore, that in comparison to other d^6 metal fragments the $CpMn(CO)_2$ system exhibits a very small effective splitting of d levels (Scheme IV), similar to Mn(II). Our studies have demonstrated the increase of the metal-centered HOMO as well as a rather low unoccupied d level (close to π^*). The reason for this situation may in part lie in the strong perturbation of octahedral symmetry around the manganese center;[23] as an additional argument for the assignments made and for the use of ESR data, it may be pointed out that the differences in g values of the anion radicals $\mathbf{10a}$–$\mathbf{c}^{-}\cdot$ correlate with photoreactivity. The pentamethylcyclopentadienyl derivative **10c** with the lowest g value (and with the largest metal hyperfine coupling!) exhibits the most pronounced photosensitivity.

Conclusions

Binuclear pyrazine-bridged complexes **10** of $CpMn(CO)_2$ fragments have been prepared and isolated despite synthetic difficulties[13b] due to slow formation and due to their propensity to dissociate into mononuclear derivatives **9** under visible light. A conspicuous property of the binuclear complexes is their deep blue color caused by a band system that is centered in the visible region of the spectrum (~2 eV). According to a combination of electron spectroscopy, cyclic voltammetry, and electron spin resonance, the low-energy transition is the consequence of a high-lying metal-centered HOMO and of a relatively low-lying ligand-centered (π^*) LUMO. The MLCT character of the first electronic transition is supported by the intensity of the bands and by their solvent dependence; additional evidence comes from high-resolution ESR spectra of the corresponding anion radicals.

Comparison with related binuclear Cr(0), Mo(0), W(0), Fe(II), Ru(II), and Os(II) complexes of pyrazine allows an assessment of the significant differences in electronic structure of such species. It turns out that the Mn(I) complexes **9** and **10** adopt an intermediate position between corresponding group 6d and group 8d complexes; their HOMO and LUMO levels are quite similar to those of analogous Ru(II) complexes while, on the other hand, their reactivity is largely determined by their less polar, organometallic character. In addition, the dissociative lability of pyrazine complexes with dicarbonylcyclopentadienylmanganese(I) fragments is strongly enhanced by visible light. Apparently, there is a photoreactive excited state lying close to or possibly below the low-lying MLCT excited state; strong evidence for such an assumption comes from the unusually small g values of the radical complexes $10^{-}\cdot$. This high photoreactivity distinguishes the Mn(I) complexes from the other d^6 metal complexes with π-electron-

---

(40) Schneider, F.; Möbius, K.; Plato, M. *Angew. Chem., Int. Ed. Engl.* **1965**, *4*, 819. Fischer, H. In "Free Radicals"; Kochi, J. K., Ed.; Wiley-Interscience: New York, 1973; Vol. II, p 452.

(41) Goodman, B. A.; Raynor, J. B. *Adv. Inorg. Chem. Radiochem.* **1970**, *13*, 136. Dunn, T. M. *Trans. Faraday Soc.* **1961**, *57*, 1441.

(42) Work in progress in cooperation with Prof. A. J. Lees, SUNY at Binghamton.

accepting N-heterocycles, a finding that provides some further aspects concerning the photochemically important control[43] of the relation between charge-transfer and ligand field excited states.

The lability of complexes **9** and **10** is also manifest in their redox chemistry. While the binuclear anion radicals $\mathbf{10}^{-\cdot}$ show some persistence in solution, the oxidative process leading to Mn(II) is highly dissociative in the presence of coordinating DMF. Nevertheless, cyclic voltammetry of the Mn(I) complexes has allowed the construction of an electron-transfer/coordination scheme (Scheme II), which exhibits several interesting features such as ECE mechanisms for the oxidation of **10** and for the reduction of **9**.

Although dissociatively stable Mn(II)/Mn(I) mixed-valence dimers could not be obtained in the study presented, the recent characterization of the first such species at −40 °C[44a] and at ambient temperature[44b] suggests that the use of stronger, possibly negatively charged ligands may lead to more organometallic mixed-valence systems.

Summarizing, the present study focusing on pyrazine-bridged Mn(I) binuclear complexes reveals several aspects concerning the possible electronic structures of such systems and demonstrates the use of the complementary physical techniques electron spectroscopy, electrochemistry, and electron spin resonance. In the absence of a detailed theoretical study of the system at hand[45] it should be pointed out that the results presented relate to recent calculations performed for the Creutz–Taube system **2**[46] and for binuclear dinitrogen complexes $N_2\cdot 2CpMn(CO)_2$,[47] both of which emphasize the crucial role of the interaction between the bridging ligand π^* level and the metal fragments for the bonding in such systems.

Acknowledgment. Work on electron-transfer reactivity of organometallics has been supported by Deutsche Forschungsgemeinschaft (DFG), Fonds der Chemischen Industrie, Flughafen Frankfurt/Main AG, and the Hermann Willkomm Foundation.

---

(43) Cf.: Caspar, J. V.; Meyer, T. J. *Inorg. Chem.* **1983**, *22*, 2444. Barigelletti, F.; Juris, F.; Balzani, V.; Belser, P.; von Zelewsky, A. *Ibid.* **1983**, *22*, 3335. Allen, G. H.; White, R. P.; Rillema, D. P.; Meyer, T. J. *J. Am. Chem. Soc.* **1984**, *106*, 2613.

(44) (a) McDonald, J. W. *Inorg. Chem.* **1985**, *24*, 1734. (b) Gross, R.; Kaim, W., unpublished results.

(45) For a general molecular orbital treatment of $CpM(CO)_2$ complexes, cf.: Schilling, B. E. R.; Hoffmann, R.; Lichtenberger, D. L. *J. Am. Chem. Soc.* **1979**, *101*, 585.

(46) Ondrechen, M. J.; Ellis, D. E.; Ratner, M. A. *Chem. Phys. Lett.* **1984**, *109*, 50.

(47) Kostić, N. M.; Fenske, R. F. *J. Organomet. Chem.* **1982**, *233*, 337.

(48) In this paper the periodic group notation is in accord with recent actions by the ACS nomenclature committee. A and B notation is eliminated because of wide confusion. Groups IA and IIA become groups 1 and 2. The d-transition elements comprise groups 3 through 12, and the p-block elements comprise groups 13 through 18. (Note that the former Roman number designation is preserved in the last digit of the new numbering: e.g., III → 3 and 13.)

Contribution from the Department of Chemistry,
University of Georgia, Athens, Georgia 30602

Chemical Applications of Topology and Group Theory. 20. Eight-Vertex Polyhedra and Their Rearrangements[1]

R. B. King

Received June 14, 1985

There are 257 combinatorially distinct eight-vertex polyhedra, of which 14 are deltahedra. Of the 14 deltahedra, only the bisdisphenoid, commonly known as the D_{2d} or triangular dodecahedron, both lacks tetrahedral chambers and can be formed by the hybridization of only s, p, and d orbitals. Degenerate single and symmetrical parallel multiple diamond–square–diamond processes involving the 14 eight-vertex deltahedra are tabulated. Among the eleven such processes (six single, two symmetrical double, one fully symmetrical triple, and two fully symmetrical quadruple), those relating the bisdisphenoid to the 4,4-bicapped trigonal prism and the square antiprism are of current chemical significance. Single, double, and quadruple dsd rearrangements of the bisdisphenoid are depicted as topologically equivalent cubes with added diagonals so that the pivot faces are faces of the underlying cube and the dsd processes involve shifting only the positions of selected diagonals without disturbing the 12 edges of the underlying cube.

Introduction

Previous papers in this series have discussed new mathematical approaches for the treatment of stereochemical nonrigidity in ML_n coordination complexes (M = central atom, generally a metal; L = ligands surrounding M) and metal clusters. Thus, Gale transformations[2] allow all possible nonplanar isomerization processes to be found for polyhedra having five and six vertices, i.e., corresponding to ML_5 and ML_6 complexes.[3] This Gale transformation approach is no longer effective for polyhedra having seven or more vertices, since Gale transforms no longer reduce the dimensionality of the problem.[4] However, the chemically based assumption[4] of minimum pivot face size in intermediate polyhedra coupled with the still manageable number of combinatorially distinct seven-vertex polyhedra, namely 34,[5] allows an exhaustive study of chemically relevant diamond–square–diamond (dsd) processes[6] in seven-vertex polyhedra.[4]

This paper presents a related treatment of polyhedral isomerizations in eight-coordinate complexes. Here the problem is considerably more complicated since there are 257 combinatorially distinct eight-vertex polyhedra (Table I).[5] In order to make the problem tractable, the following two assumptions are used:

(1) Only dsd processes (i.e., 4-pyramidal rather than *n*-pyramidal ($n \geq 5$) processes[3]) having a quadrilateral pivot face[4] will be considered. This assumption is justified on the energetic basis that polyhedra having one or more faces with five or more edges (i.e., pentagons, hexagons, heptagons, etc.) are unfavorable relative to polyhedra having only triangular and quadrilateral faces. This principle was already recognized in 1969 in the first paper of this series.[7]

(2) Only symmetrical parallel multiple dsd processes will be considered. In a symmetrical multiple dsd process the quadrilateral

---

(1) Part 19: King, R. B.; Rouvray, D. H. *Theor. Chim. Acta*, in press.

(2) Grünbaum, B. "Convex Polytopes"; Interscience: New York, 1967; Chapter 6.

(3) King, R. B. *Theor. Chim. Acta* **1984**, *64*, 439.

(4) King, R. B. *Inorg. Chem.* **1985**, *24*, 1716.

(5) Federico, P. J. *Geometriae Dedicata* **1975**, *3*, 469.

(6) Lipscomb, W. N. *Science* **1966**, *153*, 373.

(7) King, R. B. *J. Am. Chem. Soc.* **1969**, *91*, 7211.

0020-1669/86/1325-0506$01.50/0